Editors' Suggestion

Ultracold molecular collisions in magnetic fields: Efficient incorporation of hyperfine structure in the total rotational angular momentum representation

Timur V. Tscherbul [1] and Jose P. D'Incao [2]

[1] *Department of Physics, University of Nevada, Reno, Nevada 89557, USA*

[2] *JILA, National Institute of Standards and Technology, and Department of Physics, University of Colorado, Boulder, Colorado 80309, USA*

(Received 8 June 2023; accepted 30 October 2023; published 17 November 2023)

The effects of hyperfine structure on ultracold molecular collisions in external fields are largely unexplored due to major computational challenges associated with rapidly proliferating hyperfine and rotational channels coupled by highly anisotropic intermolecular interactions. We explore an efficient basis set for incorporating the effects of hyperfine structure and external magnetic fields in quantum scattering calculations on ultracold molecular collisions. The basis is composed of direct products of the eigenfunctions of the total *rotational* angular momentum (TRAM) of the collision complex J_r and the electron- and nuclear-spin basis functions of the collision partners. The separation of the rotational and spin degrees of freedom ensures rigorous conservation of J_r even in the presence of external magnetic fields and isotropic hyperfine interactions. The resulting block-diagonal structure of the scattering Hamiltonian enables coupled-channel calculations on highly anisotropic atom-molecule and molecule-molecule collisions to be performed independently for each value of J_r. We illustrate the efficiency of the TRAM basis by calculating state-to-state cross sections for ultracold He + YbF collisions in a magnetic field. The size of the TRAM basis required to reach numerical convergence is eight times smaller than that of the uncoupled basis used previously, providing a computational gain of three orders of magnitude. The TRAM basis is therefore well suited for rigorous quantum scattering calculations on ultracold molecular collisions in the presence of hyperfine interactions and external magnetic fields.

DOI: 10.1103/PhysRevA.108.053317

I. INTRODUCTION

Ultracold molecular gases offer novel opportunities for searches of new physics beyond the Standard Model [1,2], quantum information science [3–5], and quantum control of chemical reaction dynamics [6–9]. Understanding the quantum dynamics of ultracold molecular collisions is essential to realizing these opportunities by enabling the production of denser and cold molecular ensembles, and to controlling intermolecular interactions within the ensembles. This is because collisional interactions determine the properties of ultracold molecular gases, such as their stability. In particular, inelastic collisions and long-lived complex formation lead to trap loss [10,11], which limits the lifetime of trapped molecules, whereas elastic collisions result in thermalization, which is beneficial for evaporative and sympathetic cooling [1,2,12–14].

The most detailed theoretical understanding of complex molecular collisions is gained from rigorous quantum coupled-channel (CC) calculations, which solve the Schrödinger equation exactly for a given form of the interaction potential between the molecules [15,16]. Because they involve no approximations, these calculations can be used to interpret experimental observations and to relate them to the underlying microscopic interactions between the molecules [17–26]. These calculations also serve as a benchmark for approximate methods and can be used to estimate inelastic collision rates [27] and the density of scattering resonances in ultracold atom-molecule [12,13,28–30] and molecule-molecule [28] collisions.

However, acquiring such a detailed understanding of ultracold molecular collisions has been a major challenge due to the need to account for the numerous molecular degrees of freedom, which include rotational, vibrational, fine, and hyperfine structure, in addition to the interaction with external electromagnetic fields. In order to obtain numerically converged solutions of CC equations, one needs to use a very large number of molecular basis functions, which grows rapidly with the size and mass of the colliding molecules [31]. While efficient techniques have been developed for reducing the size of rotational basis sets in the absence [31,32] and in the presence [33–36] of external electromagnetic fields, there has been very little work on hyperfine basis sets.

Molecular hyperfine structure arises due to nonzero nuclear spins in one (or both) of the collision partners interacting with unpaired electrons and/or with molecular rotation [37]. These interactions result in energy-level splittings on the order of a few tens of kHz [38] to GHz [39,40], which can easily exceed the energy scale of ultracold molecular collisions ($E \leqslant 100$ kHz). Thus, hyperfine interactions are expected to profoundly affect ultracold collision dynamics by shifting and splitting collision thresholds and modifying zero-energy crossings of molecular bound states, which give rise to magnetic Feshbach resonances [41]. Indeed, with a few exceptions (such as collisions of spin-polarized species in strong magnetic fields [12–14]), it is impossible to accurately describe the magnetic-field dependence of scattering cross sections at ultralow temperatures without taking into account the hyperfine structure. The lifetimes of collision complexes may

be affected by the hyperfine structure [10,42] and strong effects of hyperfine interactions have been observed in product state distributions of the ultracold chemical reaction KRb + KRb $\rightarrow$ K_2 + Rb_2 [43,44]. Many recent experimental studies of ultracold atom-molecule [45–49] and molecule-molecule [9,50,51] collisions involve alkali-metal dimer molecules with a pronounced hyperfine structure.

These considerations strongly motivate including hyperfine interactions in rigorous CC calculations on molecular collisions in external fields. However, most of the previous calculations have neglected these interactions, as their inclusion leads to formidable computational difficulties associated with the rapid expansion of the Hilbert space. A single magnetic nucleus with spin I gives rise to a $(2I + 1)$fold increase in the number of molecular basis states, leading to a severalfold increase in the number of scattering channels. For example, in the case of cold He + YbF collisions considered in this paper, nearly converged results can be obtained with 1131 channels in the fully uncoupled basis [52–54] in the absence of hyperfine structure. Incorporating the hyperfine structure of YbF rises this number by a factor of 2, and the computational cost by a factor of 8. It is therefore not surprising why so few CC calculations on ultracold atom-molecule collisions have included hyperfine interactions. These calculations are reviewed below.

Lara *et al.* included hyperfine structure in their scattering calculations of ultracold Rb + OH collisions in the absence of external fields [55,56]. Tscherbul *et al.* performed quantum scattering calculations on He + YbF collisions in a magnetic field [54], which highlighted the importance of including hyperfine structure in CC calculations of cold and ultracold atom-molecule scattering. This work was extended to collisions of $^3\Sigma$ molecules with atoms by González-Martínez and Hutson [57]. Nuclear-spin relaxation in weakly anisotropic He + ^{13}CO collisions has recently been explored by Hermsmeier *et al.* in converged CC calculations in the temperature range 0.1–10 K [58]. Hyperfine structure was included in model CC calculations on ultracold collisions of RbCs molecules [59] and on the chemical reactions Li + CaH $\rightarrow$ LiH + Ca [60] and Na + NaLi $\rightarrow$ Na_2 + Li [49,61] in the presence of an external magnetic field. These calculations, however, used restricted CC basis sets containing only the lowest rotational states [49,61], and did not produce converged results when hyperfine interactions were included.

The vast majority of the previous CC calculations that included molecular hyperfine structure used "uncoupled" channel basis sets of the form $|f_{\rm mol}\rangle\,|lm_l\rangle$, where $|f_{\rm mol}\rangle$ are the basis functions that depend on the molecular (internal) degrees of freedom and $|lm_l\rangle$ are the partial wave basis states, which are the eigenfunctions of the orbital angular momentum squared of the collision complex $\hat{l}^2$ and of its space-fixed (SF) projection $\hat{l}_Z$. Because these basis states are not the eigenfunctions of the total angular momentum of the collision complex, they could provide converged results only for moderately anisotropic systems, such as He + YbF and Mg + NH, where only a few rotational states and partial waves are necessary to properly describe the anisotropy of the atom-molecule interaction potential. However, with the exception of collisions involving light atoms (such as He, He*, and Li) and molecules (such as H_2, CaH, NH, and O_2) [17–20,22–24,62], ultracold atom-molecule collisions studied experimentally thus far (such as Rb + CaF [63], Na + NaLi [64,65], K + NaK [45,46], and Rb + KRb [47]) are characterized by deep and strongly anisotropic interactions, which couple hundreds of rotational states at short range [13,14].

Obtaining converged results for such collisions requires the use of the total angular momentum (TAM) representation [32], which leverages the rotational invariance of intermolecular interactions to block diagonalize the scattering Hamiltonian in the absence of external fields. The TAM representation has been widely used to study ultracold atom-molecule and molecule-molecule collisions and chemical reactions under field-free conditions [7,66,67] and in the presence of external electromagnetic fields [12,13,29,33–36]. However, the hyperfine effects are yet to be incorporated in TAM calculations in the presence of external fields.

Here, we explore an alternative basis set that combines the computational efficiency of the TAM basis with the ease of evaluation of matrix elements pertinent to the fully uncoupled basis. The basis is obtained by coupling all *rotational* angular momenta in the Hamiltonian to form the total rotational angular momentum (TRAM) of the collision complex. To our knowledge, the TRAM basis was first used by Simoni and Launay [68] in their model CC calculations of ultracold Na + Na_2 collisions. More recently, similar treatments have been used for ultracold three-atom recombination reactions [69–71]. However, the calculations of Ref. [68] were performed in the absence of external fields and did not include the intramolecular spin-rotation and anisotropic hyperfine interactions, which are generally non-negligible in ultracold atom-molecule collisions [54,57]. In addition, the CC basis sets employed in Ref. [68] were too small to produce converged results, leaving the question open of whether the TRAM basis could be used for efficient CC computations on ultracold molecular collisions in magnetic fields. Here, we address this question by systematically considering all intramolecular interactions in $^2\Sigma$ molecules and performing converged CC calculations on ultracold He + YbF collisions in an external magnetic field. Our results show that the TRAM basis offers a computationally efficient way of handling hyperfine interactions in ultracold atom-molecule collisions mediated by strongly anisotropic interactions. Additional advantages of the TRAM basis include (i) the absence of unphysical states in the ground rotational manifold of the diatomic molecule and their low density in rotationally excited manifolds, and (ii) its superior computational efficiency over the TAM basis in situations, where ultracold scattering is dominated by isotropic hyperfine and Zeeman interactions. These results open up the possibility of rigorous quantum scattering calculations on ultracold atom-molecule collisions of current experimental interest [45,47,65].

The structure of this paper is as follows. In Sec. II we define the TRAM basis set and highlight its computational advantages. In Sec. III we apply the theory to calculate the cross sections for cold He + YbF collisions, a system with a pronounced hyperfine structure, which presented significant computational challenges in a previous theoretical study using an uncoupled space-fixed basis set [54]. We show how these challenges can be efficiently overcome using the TRAM basis set, leading to an order-of-magnitude reduction in the number

of coupled channels (from 1920 to 240), which translates to a nearly three-orders-of-magnitude reduction in computational effort. Section IV concludes and outlines several possible directions for future work.

II. THEORY

In this section, we define the TRAM basis set and present expressions for the matrix elements of the scattering Hamiltonian in the TRAM representation. We then discuss several computational advantages of the TRAM basis, which make it an attractive choice for quantum scattering calculations on strongly anisotropic molecular collisions in an external magnetic field in the presence of hyperfine structure. We will consider two cases of interest: collisions of $^2\Sigma$ molecules with structureless atoms, and collisions of $^2\Sigma$ molecules with atoms in electronic states of ^{2}S symmetry. Open-shell $^2\Sigma$ molecules such as SrF, CaF, or YbF have recently been laser cooled and trapped by a number of research groups [72–77]. Ultracold atom-molecule collisions are relevant for sympathetic cooling, in which molecules thermalize with an ultracold gas of atoms [12–14,78]. Recently, several experimental groups have measured the cross sections for ultracold Rb + CaF [63] and Na + NaLi collisions [48,64,65] and observed magnetic Feshbach resonances in ultracold Na + NaLi [48,49,65] and K + NaK [45,46] mixtures.

A. Collisions of $^2\Sigma$ molecules with ^{1}S$_0$ atoms

Before introducing the TRAM basis, we will briefly review the key aspects of quantum scattering theory as they apply to ultracold atom-molecule collisions in the presence of an external magnetic field. The reader is referred to Refs. [8,79] for a detailed account of the theory.

The Hamiltonian of a $^2\Sigma$ diatomic molecule colliding with a spherically symmetric ^{1}S$_0$ atom in a magnetic field may be written as (using atomic units, in which $\hbar = 1$) [33,36,52,53,79]

$$\hat{H} = -\frac{1}{2\mu R}\frac{\partial^2}{\partial R^2}R + \frac{\hat{l}^2}{2\mu R^2} + \hat{V}(r, R, \theta) + \hat{H}_{\rm mol}, \quad (1)$$

where θ is the angle between the Jacobi vectors $\mathbf{R}$ and $\mathbf{r}$, which span the configuration space of the atom-molecule collision complex, μ is the reduced mass of the triatomic complex, and $\hat{l}^2$ is the squared orbital angular momentum for the collision. The atom-molecule interaction potential $\hat{V}$ is a scalar function of the atom-molecule center-of-mass separation $R = |\mathbf{R}|$, the internuclear distance of the diatomic molecule $r = |\mathbf{r}|$, and θ. We will adopt the rigid-rotor approximation by setting $r = r_e$, where r_e is the equilibrium distance of the diatomic molecule.

Here, we focus on the simplest yet common example of hyperfine structure, which arises in $^2\Sigma$ molecules bearing a single magnetic nucleus, such as laser-coolable SrF, CaF, YbF, and YO molecules [40,72–74,80–83]. The internal structure of such molecules and their interaction with an external magnetic field are described by the Hamiltonian, which consists of three parts:

$$\hat{H}_{\rm mol} = \hat{H}^{\rm rot}_{\rm mol} + \hat{H}^{\rm spin}_{\rm mol} + \hat{H}^{\rm SR}_{\rm mol}, \quad (2)$$

where

$$\hat{H}^{\rm rot}_{\rm mol} = B_e\hat{N}^2 \quad (3)$$

is the rotational part, $\hat{\mathbf{N}}$ is the rotational angular momentum of the molecule, and B_e is the rotational constant. The spin part, which only depends on the electron- and nuclear-spin operators, is given by

$$\hat{H}^{\rm spin}_{\rm mol} = g_S\mu_0 B\hat{S}_Z + (b + c/3)\hat{\mathbf{I}}\cdot\hat{\mathbf{S}}, \quad (4)$$

where the first term on the right-hand side is the Zeeman Hamiltonian, μ_0 is the Bohr magneton, $g_S \simeq 2.0$ is the electron-spin g factor, and B is the magnitude of the external magnetic field, which defines the quantization axis of the SF coordinate frame.

In Eq. (4) $\hat{\mathbf{S}}$ and $\hat{\mathbf{I}}$ are the electron- and nuclear-spin operators [the eigenvalues of $\hat{S}^2$ are given by $S(S+1)$ with $S = 1/2$ for $^2\Sigma$ molecules]. The isotropic (or Fermi contact) hyperfine interaction [37] is given by the last term in Eq. (4), where $a = b + c/3$ is the corresponding hyperfine constant expressed via the constants b and c introduced by Frosch and Foley in Ref. [37].

The interaction Hamiltonian couples the rotational and spin degrees of freedom:

$$\hat{H}^{\rm SR}_{\rm mol} = \gamma_{\rm SR}\hat{\mathbf{N}}\cdot\hat{\mathbf{S}} + \frac{c\sqrt{6}}{3}\left(\frac{4\pi}{5}\right)^{1/2} \times \sum_{q=-2}^{2}(-1)^q Y_{2-q}(\theta_r, \phi_r)[\hat{\mathbf{I}}\otimes\hat{\mathbf{S}}]^{(2)}_q \quad (5)$$

where the electron-spin–rotation interaction $\gamma_{\rm SR}\hat{\mathbf{N}}\cdot\hat{\mathbf{S}}$ is parametrized by the coupling constant $\gamma_{\rm SR}$, and the anisotropic hyperfine interaction is parametrized by the constant c. The spherical harmonics Y_{2-q} depend on the angles θ_r and ϕ_r, which specify the orientation of the molecular axis in the SF frame. We neglect the nuclear spin-rotational interaction $C\hat{\mathbf{I}}\cdot\hat{\mathbf{N}}$, which for YbF is three orders of magnitude smaller than the electron-spin–rotation interaction [54].

As illustrated in Fig. 1, the commuting operators $\hat{H}^{\rm rot}_{\rm mol}$ and $\hat{H}^{\rm spin}_{\rm mol}$ act in different subspaces of the total Hilbert space of the molecule, which is a direct product of rotational and spin subspaces (with the latter including both the electron- and nuclear-spin subspaces).

Our goal is to solve the time-independent Schrödinger equation $\hat{H}|\Psi\rangle = E|\Psi\rangle$ with the Hamiltonian given by Eq. (1). To this end we expand the solution at fixed total energy E in channel functions $|\Phi_n\rangle$:

$$|\Psi\rangle = \frac{1}{R}\sum_n F_n(R)|\Phi_n\rangle, \quad (6)$$

where $F_n(R)$ are the radial functions, which satisfy the standard CC equations (in atomic units, $\hbar = 1$)

$$\left[\frac{d^2}{dR^2} + 2\mu E\right]F_n(R) = 2\mu\sum_{n'}\langle\Phi_n|\hat{V}(R,\theta) + \frac{\hat{l}^2}{2\mu R^2} + \hat{H}_{\rm mol}|\Phi_{n'}\rangle F_{n'}(R). \quad (7)$$

The asymptotic behavior of the radial functions defines the scattering S matrix, from which all scattering observables can

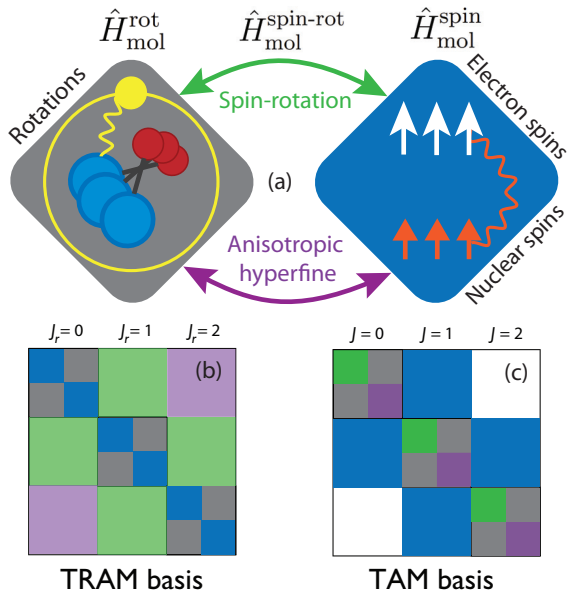

FIG. 1. (a) Schematic representation of the total molecular Hilbert space as a direct product of two subspaces corresponding to molecular rotations (left diamond) and to the electron- and nuclear-spin degrees of freedom (right diamond). The yellow and orange wavy lines represent, respectively, the anisotropy of the electrostatic atom-molecule interaction potential (left diamond) and the isotropic (Fermi contact) hyperfine interaction (right diamond). Matrix representation of the molecular Hamiltonian in the TRAM basis (b) and in the TAM basis (c). The color coding scheme is as follows: gray, rotational kinetic energy and adiabatic interaction potential; blue, isotropic hyperfine and Zeeman interactions; green and violet, electron-spin–rotation interaction and anisotropic hyperfine interactions.

be obtained, including differential and integral cross sections, transition rates, and collision lifetimes.

1. Matrix elements in the TRAM basis: Intramolecular rotational, hyperfine, and Zeeman interactions

We expand the solution of the time-independent Schrödinger equation (6) in a space-fixed TRAM basis:

$$|\Phi_n\rangle = |(Nl)J_rM_r\rangle|n_s\rangle, \tag{8}$$

where $|(Nl)J_rM_r\rangle$ are the eigenstates of the TRAM of the collision complex $\hat{\mathbf{J}}_r = \hat{\mathbf{N}} + \hat{\mathbf{l}}$, and its projection on the Z axis $\hat{J}_{r_Z}$, and $|n_s\rangle$ are the basis functions for the electron- and nuclear-spin degrees of freedom (see below).

The eigenstates of $\hat{J}_r^2$ and $\hat{J}_{r_Z}$ are obtained by coupling the eigenstates of $\hat{N}^2$ and $\hat{N}_Z$ and those of $\hat{l}^2$ and $\hat{l}_Z$ [84]:

$$|(Nl)J_rM_r\rangle = \sum_{M_N,m_l} \langle NM_N lm_l|J_rM_r\rangle |NM_N\rangle|lm_l\rangle, \tag{9}$$

where $|lm_l\rangle$ are the eigenstates of $\hat{l}^2$ and $\hat{l}_Z$, $|NM_N\rangle$ are those of $|\hat{\mathbf{N}}|^2$ and $\hat{N}_Z$, and $\langle j_1m_1j_2m_2|jm\rangle$ are the Clebsch-Gordan coefficients. Note that $\hat{\mathbf{J}}_r = \hat{\mathbf{N}} + \hat{\mathbf{l}}$ is different from the total angular momentum operator $\hat{\mathbf{J}} = \hat{\mathbf{N}} + \hat{\mathbf{l}} + \hat{\mathbf{S}} + \hat{\mathbf{I}} = \hat{\mathbf{J}}_r + \hat{\mathbf{S}} + \hat{\mathbf{I}}$ unless $I = S = 0$.

Below we will evaluate the matrix elements of the scattering Hamiltonian in the TRAM basis. We also discuss the structure of the coupling matrix elements, which makes clear the unique advantages offered by this basis for incorporating hyperfine structure and magnetic fields in quantum scattering calculations on molecular collisions in external fields.

We begin with the Hamiltonian of the diatomic molecule (2). Taking advantage of the structure of the TRAM basis, which is a direct product of basis functions for the rotational and spin degrees of freedom, we find

$$\begin{aligned}\langle (Nl)J_rM_r|\langle n_s|\hat{H}_{\rm mol}|(N'l')J_r'M_r'\rangle|n_s'\rangle \\ = \delta_{n_sn_s'}\langle (Nl)J_rM_r|\hat{H}^{\rm rot}_{\rm mol}|(N'l')J_r'M_r'\rangle \\ + \delta_{NN'}\delta_{ll'}\delta_{J_rJ_r'}\delta_{M_rM_r'}\langle n_s|\hat{H}^{\rm spin}_{\rm mol}|n_s'\rangle \\ + \langle (Nl)J_rM_r|\langle n_s|\hat{H}^{\rm SR}_{\rm mol}|(N'l')J_r'M_r'\rangle|n_s'\rangle. \end{aligned}\tag{10}$$

We observe that the purely rotational part of the Hamiltonian $\hat{H}^{\rm rot}_{\rm mol}$ is diagonal in the spin degrees of freedom, whereas the spin part $\hat{H}^{\rm spin}_{\rm mol}$ (including the Zeeman interaction) is diagonal in the rotational degrees of freedom, as expected. The spin-rotation interaction $\hat{H}^{\rm SR}_{\rm mol}$ couples the rotational and spin degrees of freedom.

To proceed, we need to specify the basis ket vectors $|n_s\rangle$ for the spin degrees of freedom. Here, as in our previous work [54], we use the fully uncoupled spin basis set $|n_s\rangle = |SM_S\rangle\,|IM_I\rangle$, although the coupled hyperfine basis $|n_s\rangle = |Fm_F\rangle$ could be used as well. The first term on the right-hand side of Eq. (10) is diagonal since the basis states $|(Nl)J_rM_r\rangle$ are eigenstates of $\hat{N}^2$:

$$\begin{aligned}\langle (Nl)J_rM_r|\langle SM_S|\langle IM_I|\hat{H}^{\rm rot}_{\rm mol}|(N'l')J_r'M_r'\rangle|SM_S'\rangle|IM_I'\rangle \\ = \delta_{M_IM_I'}\delta_{M_SM_S'}\delta_{NN'}\delta_{ll'}\delta_{J_rJ_r'}\delta_{M_rM_r'}B_eN(N+1). \end{aligned}\tag{11}$$

The matrix element of $\hat{H}^{\rm spin}_{\rm mol} = a\hat{\mathbf{I}}\cdot\hat{\mathbf{S}} + g_S\mu_0B\hat{S}_Z$ in the second term is straightforward to derive since our spin basis states $|SM_S\rangle|IM_I\rangle$ are eigenstates of $\hat{S}_Z$ and $\hat{I}_Z$, and thus [see, e.g., Eq. (7) of Ref. [54]]

$$\begin{aligned}\langle (Nl)J_rM_r|\langle SM_S|\langle IM_I|a\hat{\mathbf{I}}\cdot\hat{\mathbf{S}}|(N'l')J_r'M_r'\rangle|SM_S'\rangle|IM_I'\rangle \\ = \delta_{NN'}\delta_{ll'}\delta_{J_rJ_r'}\delta_{M_rM_r'}a[\delta_{M_IM_I'}\delta_{M_SM_S'}M_IM_S \\ + \tfrac{1}{2}\delta_{M_I,M_I'\pm1}\delta_{M_S,M_S'\mp1}C_\pm(I,M_I')C_\mp(S,M_S')] \end{aligned}\tag{12}$$

where $C_\pm(J,M) = [J(J+1) - M(M\pm1)]^{1/2}$. Note that the spin Hamiltonian $\hat{H}^{\rm spin}_{\rm mol}$ is diagonal in J_r because the isotropic hyperfine and Zeeman interactions do not act on the rotational degrees of freedom. This is a key difference between the TRAM basis and the more familiar total angular momentum basis, in which the Zeeman interaction couples basis states with different J [33,36].

Finally, the spin-rotation coupling matrix element [the third term in Eq. (10)] is the sum of the matrix elements of the electron-spin–rotation interaction $\hat{H}^{\rm ESR}_{\rm mol} = \gamma_{\rm SR}\hat{\mathbf{N}}\cdot\hat{\mathbf{S}}$ and of the anisotropic hyperfine interaction $\hat{H}^{\rm AHF}_{\rm mol} = \frac{c\sqrt{6}}{3}(\frac{4\pi}{5})^{1/2}\sum_{q=-2}^{2}(-1)^qY_{2-q}(\theta_r,\phi_r)[\hat{\mathbf{I}}\otimes\hat{\mathbf{S}}]^{(2)}_q$ [see Eq. (5)].

The matrix elements of the electron-spin–rotation interaction in the TRAM basis are given by (see Appendix A)

$$\langle (Nl)J_rM_r|\langle SM_S|\langle IM_I|\hat{H}^{\rm ESR}_{\rm mol}|(N'l')J'_rM'_r\rangle|SM'_S\rangle|IM'_I\rangle = \delta_{M_IM'_I}\delta_{ll'}\delta_{NN'}\gamma_{\rm SR}p_3(N)p_3(S)[(2J_r+1)(2J'_r+1)]^{1/2} \times \sum_p (-1)^p(-1)^{J_r-M_r}(-1)^{N+l+J'_r+1}(-1)^{S-M_S}\begin{Bmatrix} N & J_r & l \\ J'_r & N & 1\end{Bmatrix} \times \begin{pmatrix} J_r & 1 & J'_r \\ -M_r & p & M'_r\end{pmatrix}\begin{pmatrix} S & 1 & S \\ -M_S & -p & M'_S\end{pmatrix} \tag{13}$$

where $p_3(X) = [(2X+1)X(X+1)]^{1/2}$. It follows from Eq. (13) that the electron-spin–rotation interaction couples TRAM basis states with $J_r - J'_r = \pm 1$. This interaction conserves the value of $M_r + M_S$ as well as the total angular momentum projection $M = M_r + M_S + M_I$. This coupling is typically much weaker than either the rotational energy scale or the Zeeman interaction at moderate and high magnetic fields. Nevertheless, it plays an important role in collisions of $^2\Sigma$ molecules with structureless atoms [17,53]. In order to account for this interaction, it is therefore necessary to include at least two J_r blocks ($J_r = 0{-}1$ for the initial $N = 0$ states).

The matrix elements of the intramolecular anisotropic hyperfine interaction take the form (see Appendix B)

$$\begin{aligned}&\langle (Nl)J_rM_r|\langle SM_S|\langle IM_I|\hat{H}^{\rm AHF}_{\rm mol}|(N'l')J'_rM'_r\rangle|SM'_S\rangle|IM'_I\rangle \\ &= \delta_{ll'}c\frac{\sqrt{30}}{3}(-1)^{J_r-M_r+l+J'_r}p_3(I)p_3(S)[(2J_r+1)(2J'_r+1)]^{1/2} \\ &\times[(2N+1)(2N'+1)]^{1/2}\begin{Bmatrix} N & J_r & l \\ J'_r & N' & 2\end{Bmatrix}\begin{pmatrix} 1 & 1 & 2 \\ M_I-M'_I & M_S-M'_S & M_r-M'_r\end{pmatrix} \\ &\times\begin{pmatrix} J_r & 2 & J'_r \\ -M_r & M_r-M'_r & M'_r\end{pmatrix}\begin{pmatrix} N & 2 & N' \\ 0 & 0 & 0\end{pmatrix}\begin{pmatrix} I & 1 & I \\ -M_I & M_I-M'_I & M'_I\end{pmatrix}\begin{pmatrix} S & 1 & S \\ -M_S & M_S-M'_S & M'_S\end{pmatrix}.\end{aligned} \tag{14}$$

The anisotropic hyperfine interaction couples the states with $J_r - J'_r = \pm 2$ and with $N - N' = \pm 2$ but conserves the total angular momentum projection M. Thus, in order to account for this interaction, it is necessary to include at least three lowest J_r blocks ($J_r = 0$–2 for the initial $N = 0$ states).

The spectroscopic constants of YbF($^2\Sigma$) are (in units of cm^{-1}) $c = 2.848\,75 \times 10^{-3}$, $\gamma_{\rm SR} = 4.4778 \times 10^{-4}$, $b = 4.729\,83 \times 10^{-3}$, and $B_e = 0.241\,29$. The anisotropic hyperfine interaction is thus 6.4 times stronger than the electron-spin–rotation interaction, but two times weaker than the isotropic (Fermi contact) hyperfine interaction parametrized by $a = b + c/3 = 5.6794 \times 10^{-3}$ cm^{-1}.

2. *Matrix elements in the TRAM basis: Orbital angular momentum and interaction potential*

To complete the parametrization of CC Eqs. (7) in the TRAM basis, we need to evaluate the matrix elements of the centrifugal kinetic energy and of the atom-molecule interaction potential. As the TRAM basis functions (8) are eigenfunctions of $\hat{l}^2$, the centrifugal kinetic energy has only diagonal matrix elements:

$$\begin{aligned}&\langle (Nl)J_rM_r|\langle n_s|\frac{\hat{l}^2}{2\mu R^2}|(N'l')J'_rM'_r\rangle|n'_s\rangle \\ &= \delta_{NN'}\delta_{ll'}\delta_{J_rJ'_r}\delta_{M_rM'_r}\delta_{n_sn'_s}\frac{l(l+1)}{2\mu R^2}.\end{aligned} \tag{15}$$

The adiabatic interaction potential between a $^2\Sigma$ molecule and a ^1S atom is independent of the electron and nuclear spins, so its matrix elements are diagonal in n_s. Expanding the potential in Legendre polynomials as $V(R,\theta) = \sum_\lambda V_\lambda(R)P_\lambda(\cos\theta)$ and using the Wigner-Eckart theorem, we find the matrix elements [85]:

$$\begin{aligned}&\langle (Nl)J_rM_r|\langle n_s|V(R,\theta)|(N'l')J'_rM'_r\rangle|n'_s\rangle \\ &= \delta_{n_sn'_s}\delta_{J_rJ'_r}\delta_{M_rM'_r}(-1)^{J_r+N+N'}[(2N+1)(2N'+1) \\ &\times(2l+1)(2l'+1)]^{1/2}\sum_\lambda V_\lambda(R)\begin{Bmatrix} N & l & J \\ l' & N' & \lambda\end{Bmatrix} \\ &\times\begin{pmatrix} N & \lambda & N' \\ 0 & 0 & 0\end{pmatrix}\begin{pmatrix} l & \lambda & l' \\ 0 & 0 & 0\end{pmatrix}.\end{aligned} \tag{16}$$

The matrix elements are diagonal in J_r. Because the couplings between the different J_r blocks due to the spin-rotation interactions are weak (see the previous section), the scattering Hamiltonian is approximately block diagonal in the TRAM representation as shown in Fig. 1(b). Thus, one might expect that numerical solutions of CC equations may be efficiently obtained with only the few lowest J_r blocks retained in the basis. As shown in Sec. III below, this expectation turns out to be true. This advantage of the TRAM basis is similar to that provided by the total angular momentum representation [33,35].

The matrix elements (16) have a simple form, which does not increase in complexity as additional hyperfine or electron-spin degrees of freedom are added. The underlying reason for this simplicity is that in the TRAM representation one only couples the *rotational* angular momenta, on which the interaction potential actually depends. By contrast, in the space-fixed TAM representation, one needs to couple *all* angular momenta regardless of whether or not they are coupled by the interaction potential, leading to a nested hierarchy of partially coupled basis functions, whose complexity increases rapidly as more angular momenta are added [35,36].

B. Collisions of $^2\Sigma$ molecules with ^{2}S atoms

The Hamiltonian of the collision complex formed by a $^2\Sigma$ molecule and an $^2S_0$ atom may be written as

$$\hat{H} = -\frac{1}{2\mu R}\frac{\partial^2}{\partial R^2}R + \frac{\hat{l}^2}{2\mu R^2} + \hat{V}_{\rm int} + \hat{H}_{\rm mol} + \hat{H}_{\rm atom} + \hat{V}_{\rm MDD}, \tag{17}$$

where all the terms except for the interaction potential operator $\hat{V}_{\rm int}$ and the new terms $\hat{H}_{\rm atom}$ and $\hat{V}_{\rm MDD}$ (see below) have the same meaning as in Eq. (1). The Hamiltonian (17) differs from Eq. (1) in three significant respects.

First, the $^2S_{1/2}$ atomic collision partner (such as an alkali-metal atom) has internal structure described by the hyperfine-Zeeman Hamiltonian

$$\hat{H}_{\rm atom} = g_S\mu_0 B\hat{S}_{a_Z} + A_a\hat{\mathbf{I}}_a\cdot\hat{\mathbf{S}}_a, \tag{18}$$

where $\hat{\mathbf{S}}_a$ and $\hat{\mathbf{I}}_a$ are the atomic electron- and nuclear-spin operators, and A_a is the atomic hyperfine constant. For simplicity, we will neglect the dependence of atomic and molecular hyperfine constants on R, r, and θ as well as tensor hyperfine couplings of the form $\hat{\mathbf{S}}\cdot\mathsf{T}(R,\theta,r)\cdot\hat{\mathbf{I}}_a$, where $\mathsf{T}(R,\theta,r)$ is a second-rank tensor that describes the coupling of the molecule's electron spin with the nuclear spin of the atom. Other forms of the tensor hyperfine coupling are possible, such as $\hat{\mathbf{S}}_a\cdot\mathsf{T}_a(R,\theta,r)\cdot\hat{\mathbf{I}}$, which describes the coupling of the atom's electron spin with the nuclear spin of the diatomic molecule. These expressions can be expanded in either Cartesian or spherical tensor products (see Refs. [86,87] for more details). While these tensor interactions are typically weaker than those already included in Eqs. (2) and (18) (see, e.g., Refs. [88,89]), they can become substantial in the short-range collision complex region [90]. These interactions can be handled by evaluating their matrix elements in the TRAM basis, and will result in additional mixing between the states of different J_r similar in form to the couplings induced by the magnetic dipole-dipole interaction as described below.

Second, the interaction potential between a $^2\Sigma$ molecule and a ^{2}S atom is no longer a single scalar function of the internal coordinates R, r, and θ as was the case for interactions with structureless atoms (see Sec. II A), but depends on the eigenvalues $S_T(S_T+1)$ of $\hat{S}_T^2$, where $\hat{\mathbf{S}}_T = \hat{\mathbf{S}} + \hat{\mathbf{S}}_a$ is the total spin of the atom-molecule collision complex [13]:

$$\hat{V}_{\rm int} = \sum_{S_T,M_{S_T}} V^{S_T}(R,r,\theta)|S_TM_{S_T}\rangle\langle S_TM_{S_T}| \tag{19}$$

where $V_{S_T}(R,r,\theta)$ are the adiabatic potential-energy surfaces (PESs) for the singlet ($S_T=0$) and triplet ($S_T=1$) electronic states. These PESs are typically very different at short range, where strong exchange interactions lead to large singlet-triplet energy gaps, as in the case of two interacting hydrogen or alkali-metal atoms [41,91].

Finally, the magnetic dipole-dipole interaction between the electron spins of the open-shell collision partners takes the form [13,35,53,92]

$$\hat{V}_{\rm MDD} = -\left(\frac{24\pi}{5}\right)^{1/2}\frac{\alpha^2}{R^3}\sum_q(-1)^q Y_{2,-q}(\hat{R})[\hat{\mathbf{S}}\otimes\hat{\mathbf{S}}_a]^{(2)}_q \tag{20}$$

where the spherical harmonic $Y_{2,-q}(\hat{R})$ depends on the orientation of vector $\hat{R}=\mathbf{R}/R$ in the space-fixed frame, and $[\hat{\mathbf{S}}\otimes\hat{\mathbf{S}}_a]^{(2)}_q$ is a second-rank tensor product of the molecular and atomic electron-spin operators.

The TRAM basis for collisions of $^2\Sigma$ molecules with ^{2}S atoms is a direct product of basis states for the structureless atom collision problem [Eq. (8)] with atomic spin basis functions $|n_s^{(a)}\rangle$:

$$|\Phi_n\rangle = |(Nl)J_rM_r\rangle|n_s\rangle|n_s^{(a)}\rangle. \tag{21}$$

As before, we choose the molecular and atomic spin basis functions in the uncoupled angular momentum representation [52,53]:

$$\begin{aligned}|n_s\rangle &= |SM_S\rangle|IM_I\rangle = |SM_SIM_I\rangle,\\ \left|n_s^{(a)}\right\rangle &= |S_aM_{S_a}\rangle|I_aM_{I_a}\rangle = |S_aM_{S_a}I_aM_{I_a}\rangle.\end{aligned} \tag{22}$$

Alternatively, one could use a coupled representation, where $|n_s\rangle = |(IS)FM_F\rangle$ and $|n_s^{(a)}\rangle = |(I_aS_a)F_aM_{F_a}\rangle$.

The matrix elements of the molecular Hamiltonian (2) and of the centrifugal kinetic energy are diagonal in atomic spin quantum numbers $n_s^{(a)}$. The expressions for these matrix elements are identical to those already presented in Sec. II A. We now proceed to evaluate the matrix elements of the three remaining terms (18)–(20).

The matrix elements of the atomic Hamiltonian are diagonal in all molecular quantum numbers:

$$\begin{aligned}&\langle(Nl)J_rM_r\langle n_s\left|\langle n_s^{(a)}\right|\hat{H}_{\rm atom}|(N'l')J_r'M_r'\rangle|n_s'\rangle\left|n_s^{(a)\prime}\right\rangle\\ &\quad= \delta_{NN'}\delta_{ll'}\delta_{J_rJ_r'}\delta_{M_rM_r'}\delta_{n_sn_s'}\left\langle n_s^{(a)}\right|\hat{H}_{\rm atom}\left|n_s^{(a)\prime}\right\rangle.\end{aligned} \tag{23}$$

Choosing the fully uncoupled representation for the atomic basis functions, the right-hand side evaluates to, in close analogy with Eq. (12),

$$\begin{aligned}\langle S_aM_{S_a}|\langle I_aM_{I_a}|\hat{H}_{\rm atom}|S_aM_{S_a}'\rangle|I_aM_{I_a}'\rangle &= \delta_{M_{I_a}M_{I_a}'}\delta_{M_{S_a}M_{S_a}'}g_S\mu_0BM_{S_a} + A_a\big[\delta_{M_{I_a}M_{I_a}'}\delta_{M_{S_a}M_{S_a}'}M_IM_S\\ &\quad+\tfrac{1}{2}\delta_{M_{I_a},M_{I_a}'\pm1}\delta_{M_{S_a},M_{S_a}'\mp1}C_\pm(I_a,M_{I_a}')C_\mp(S_a,M_{S_a}')\big].\end{aligned} \tag{24}$$

The interaction potential between a $^2\Sigma$ molecule and a ^{2}S atom is expressed in terms of projectors on eigenstates of the total electron spin $|S_TM_T\rangle$ of the atom-molecule system (19). Its matrix elements in the TRAM basis factorize into the rotational and electron-spin parts:

$$\begin{aligned}&\langle(Nl)J_rM_r|\langle SM_SIM_I|\langle S_aM_{S_a}I_aM_{I_a}|\hat{V}_{\rm int}|(N'l')J_r'M_r'\rangle|SM_S'IM_I'\rangle S_aM_{S_a}'I_aM_{I_a}'\rangle\\ &\quad= \delta_{M_IM_I'}\delta_{M_{I_a}M_{I_a}'}\sum_{S_T,M_{S_T}}\langle(Nl)J_rM_r|\langle n_s|V^{S_T}(R,r,\theta)|(N'l')J_r'M_r'\rangle\langle SM_S|\langle S_aM_{S_a}|S_TM_{S_T}\rangle\langle S_TM_{S_T}|S'M_S'\rangle|S_aM_{S_a}'\rangle.\end{aligned} \tag{25}$$

The total spin eigenfunctions are expressed in terms of the uncoupled spin functions as $|S_T M_{S_T}\rangle = \sum_{M_S} \langle SM_S, S_a M_{S_a} | SM_{S_T}\rangle |SM_S\rangle |S_a M_{S_a}\rangle$ [53]. Multiplying the Hermitian conjugate of this expression by $|SM'_S\rangle |S'_a M'_{S_a}\rangle$ and integrating over the spin degrees of freedom, the spin overlaps in Eq. (25) can be expressed in terms of the Clebsch-Gordan coefficients, e.g., $\langle S_T M_{S_T} | S' M'_S\rangle |S_a M'_{S_a}\rangle = \langle SM'_S, S_a M'_{S_a} | S_T M_{S_T}\rangle$. Substituting the rotational matrix elements of $V^S(R,\theta,r)$ from Eq. (16), we obtain the final result:

$$\begin{aligned}
&\langle (Nl) J_r M_r | \langle SM_S I M_I | \langle S_a M_{S_a} I_a M_{I_a} | \hat{V}_{\rm int} | (N'l') J'_r M'_r\rangle | SM'_S I M'_I\rangle | S_a M'_{S_a} I_a M'_{I_a}\rangle \\
&\quad = \delta_{M_I M'_I} \delta_{M_{I_a} M'_{I_a}} \delta_{J_r J'_r} \delta_{M_r M'_r} (-1)^{J_r+N+N'} [(2N+1)(2N'+1)(2l+1)(2l'+1)]^{1/2} \sum_{S_T, M_{S_T}} (-1)^{2(S-S_a+M_{S_T})} (2S_T+1) \\
&\quad \times \begin{pmatrix} S & S_a & S_T \\ M_S & M_{S_a} & -M_{S_T} \end{pmatrix} \begin{pmatrix} S & S_a & S_T \\ M'_S & M'_{S_a} & -M_{S_T} \end{pmatrix} \sum_\lambda V_\lambda^{S_T}(R,r) \begin{Bmatrix} N & l & J \\ l' & N' & \lambda \end{Bmatrix} \begin{pmatrix} N & \lambda & N' \\ 0 & 0 & 0 \end{pmatrix} \begin{pmatrix} l & \lambda & l' \\ 0 & 0 & 0 \end{pmatrix},
\end{aligned} \tag{26}$$

where the spin-dependent Legendre expansion coefficients are defined by $V^{S_T}(R,\theta,r) = \sum_\lambda V_\lambda^{S_T}(R,r) P_\lambda(\cos\theta)$ for each $S_T = |S - S_a|, \ldots, S + S_a$. The matrix of the electrostatic interaction potential is diagonal in J_r, which is significant because the anisotropic atom-molecule interactions can be block diagonalized, enabling the scattering problem to be solved independently for each J_r even in the presence of the Zeeman and isotropic hyperfine interactions (since, as shown above, these interactions are diagonal in J_r). The only interactions that couple the states of different J_r are the spin-rotation interactions (see above and Fig. 1), which are weak, so only a few values of J_r are sufficient to achieve numerical convergence of scattering observables, as demonstrated below.

The interaction potential matrix is also diagonal in the atomic and molecular nuclear-spin projections, since the potential does not depend on the nuclear-spin operators. The interaction potential couples the states with different M_S and M_{S_a} and the same $M_S = M_S + M_{S_a}$ due to the difference between the potentials with different S_T at short range (this is analogous to the spin-exchange interaction in alkali-metal dimers). The only exceptions are the states with the maximum possible M_S and M_{S_a}, which correspond to the fully stretched basis states $|S, M_S = S\rangle$ and $|S_a, M_{S_a} = S\rangle$ with $S_T = S + S_a$. These states occur in collisions of fully spin-polarized molecules and/or atoms, whose collision dynamics can often be adequately described by a single, high-spin PES [13,35].

Finally, the magnetic dipolar interaction is a contraction of tensor operators (20), which depend on the orientation of the atom-molecule axis in the SF frame [via the term $Y_{2,-q}(\hat{R})$] and on the spin degrees of freedom [via the term $[\hat{\mathbf{S}} \otimes \hat{\mathbf{S}}_a]_q^{(2)}$]. The matrix element of Eq. (20) in the TRAM basis then takes the form

$$\begin{aligned}
&\langle (Nl) J_r M_r | \langle SM_S I M_I | \langle S_a M_{S_a} I_a M_{I_a} | \hat{V}_{\rm MDD} | (N'l') J'_r M'_r\rangle | SM'_S I M'_I\rangle | S_a M'_{S_a} I_a M'_{I_a}\rangle \\
&\quad = -\left(\frac{24\pi}{5}\right)^{1/2} \frac{\alpha^2}{R^3} \delta_{M_I M'_I} \delta_{M_{I_a} M'_{I_a}} \sum_q (-1)^q \langle (Nl) J_r M_r | Y_{2,-q}(\hat{R}) | (N'l') J'_r M'_r\rangle \langle SM_S | \langle S_a M_{S_a} | [\hat{\mathbf{S}} \otimes \hat{\mathbf{S}}_a]_q^{(2)} | SM'_S\rangle | S_a M'_{S_a}\rangle.
\end{aligned} \tag{27}$$

Using the definition of the tensor product [84] to evaluate the matrix element of $[\hat{\mathbf{S}} \otimes \hat{\mathbf{S}}_a]_q^{(2)}$ and then applying the Wigner-Eckart theorem, one obtains (see Appendix C)

$$\begin{aligned}
&\langle (Nl) J_r M_r | \langle SM_S I M_I | \langle S_a M_{S_a} I_a M_{I_a} | \hat{V}_{\rm MDD} | (N'l') J'_r M'_r\rangle | SM'_S I M'_I\rangle | S_a M'_{S_a} I_a M'_{I_a}\rangle \\
&\quad = \frac{-\sqrt{30}\alpha^2}{R^3} \delta_{M_I M'_I} \delta_{M_{I_a} M'_{I_a}} \delta_{NN'} (-1)^{2J_r - M_r + N + l' + l} [(2J_r+1)(2J'_r+1)]^{1/2} \begin{pmatrix} J_r & 2 & J'_r \\ -M_r & M_r - M'_r & M'_r \end{pmatrix} \begin{Bmatrix} l & J_r & N \\ J'_r & l' & 2 \end{Bmatrix} \\
&\quad \times [(2l+1)(2l'+1)]^{1/2} \begin{pmatrix} l & 2 & l' \\ 0 & 0 & 0 \end{pmatrix} p_3(S) p_3(S_a) \begin{pmatrix} 1 & 1 & 2 \\ M_S - M'_S & M_{S_a} - M'_{S_a} & M_r - M'_r \end{pmatrix} (-1)^{S - M_S + S_a - M_{S_a}} \\
&\quad \times \begin{pmatrix} S & 1 & S \\ -M_S & M_S - M'_S & M'_S \end{pmatrix} \begin{pmatrix} S_a & 1 & S_a \\ -M_{S_a} & M_{S_a} - M'_{S_a} & M'_{S_a} \end{pmatrix}.
\end{aligned} \tag{28}$$

The magnetic dipolar interaction is seen to be diagonal in the nuclear-spin quantum numbers and to couple the TRAM basis states with values of J_r differing by 2. The minimum TRAM basis for the magnetic dipolar interaction should therefore contain at least three J_r blocks ($J_r = 0$–2 for the initial $N = 0$ states) as in the case of the anisotropic hyperfine interaction considered above. Unlike the atom-molecule interaction potential, the magnetic dipolar interaction does not separately conserve the rotational and spin angular momentum projections M_r, M_S, and M_{S_a}, but does conserve the sum $M_S + M_{S_a} + M_r$.

We now summarize the key advantages of the TRAM basis, which follow from the above discussion.

(1) Most of the terms in the scattering Hamiltonian, including the interaction potential (16), the interaction of the molecule and atom with an external magnetic field, and the isotropic hyperfine interaction [Eqs. (2) and (18)], are diagonal in the TRAM quantum number J_r. Thus, the atom-molecule scattering Hamiltonian is strongly diagonally dominant in the TRAM representation as shown in Fig. 1(a). While this nearly block-diagonal structure is superficially similar to the one which occurs in the TAM basis [33,36],

there are important differences. Specifically, the Zeeman interaction is the only interaction which is nondiagonal in J [33,36].

(2) Couplings between the different values of J_r arise *only* due to the interaction of molecular rotations with the electron and/or nuclear spins. These interactions can originate either from within the diatomic molecule, due to the spin-rotation interaction (5), or from the intramolecular magnetic dipole-dipole interaction. These couplings are typically weak.

(3) Because of the nearly block-diagonal structure of the Hamiltonian in the TRAM basis, one might expect that efficient numerical solutions of CC equations may be obtained with only the few lowest J_r blocks retained in the basis. As shown in Sec. III below, this expectation turns out to be true. This is a key advantage of the TRAM basis, which allows efficient handling of strongly anisotropic interactions. This advantage is similar to that provided by the total angular momentum basis [33,35].

III. RESULTS

In this section, we apply the TRAM representation developed in the previous section to calculate the cross sections for ultracold collisions between YbF($^2\Sigma$) molecules and He atoms in the presence of an external magnetic field. YbF is of interest for precision searches for the electric dipole moment of the electron [93], and it has recently been laser cooled [75]. YbF has a pronounced hyperfine structure, whose marked effect on cold and ultracold He + YbF collisions was studied in our previous work using a fully uncoupled angular momentum basis [54]. These calculations provide a convenient benchmark, against which we will test our TRAM approach.

A. Hyperfine-Zeeman energy levels and unphysical states

Figure 2 shows the lowest hyperfine-Zeeman energy levels of YbF($^2\Sigma$) as a function of magnetic field. The physical energy levels shown by straight lines are obtained by diagonalization of the isolated YbF Hamiltonian (2) in the single-molecule basis $|NM_N\rangle|SM_S\rangle|IM_I\rangle$. The eigenvalues of the same Hamiltonian in the TRAM basis obtained by diagonalizing the matrix in Eq. (10) are shown by symbols. We note that these sets of levels are not necessarily identical because the spin-rotation and anisotropic hyperfine interactions couple the states of different J_r (see Fig. 1). Since our TRAM basis is truncated at a finite value of $J_r^{\max}$, the couplings between the J_rth and (J_r+1)th blocks are excluded from consideration, leading to the appearance of unphysical energy levels, just as in the case of the TAM representation [33,34,36].

In further analogy with the unphysical states that occur in the TAM representation [33,34,36], the eigenvectors of the unphysical states are dominated by contributions from the highest value of J_r included in the TRAM basis. Consider, e.g., the unphysical state with the largest deviation from any physical hyperfine-Zeeman state in the $N=1$ manifold. This state is marked by an arrow in Fig. 2 and its eigenvector can be expanded in the TRAM basis states $|J_r, M_r, M_I, M_S\rangle$ at

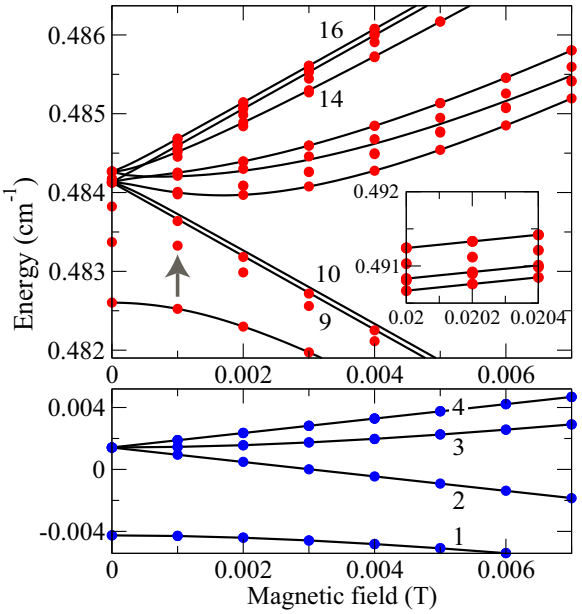

FIG. 2. Hyperfine-Zeeman energy levels in the ground ($N=0$, bottom) and the first rotationally excited ($N=1$, top) manifolds of YbF($^2\Sigma$) plotted as a function of magnetic field. Solid lines, physical hyperfine-Zeeman levels; circles, eigenvalues of the molecular Hamiltonian in the TRAM basis calculated for $N^{\max}=4$, $J_r^{\max}=2$, and $M=1$. The inset shows a portion of the energy-level spectra at higher fields. For $N=0$ the deviation of the eigenvalues of the asymptotic Hamiltonian in the TRAM basis from the physical hyperfine-Zeeman levels of YbF ($\leqslant 0.01\%$) is much less than the size of the symbols.

$B = 10^{-3}$ T:

$$|u\rangle = 0.83\left|2, 2, -\tfrac{1}{2}, -\tfrac{1}{2}\right\rangle - 0.31\left|2, 0, \tfrac{1}{2}, \tfrac{1}{2}\right\rangle + 0.225\left|1, 1, \tfrac{1}{2}, -\tfrac{1}{2}\right\rangle + \cdots, \quad (29)$$

where the quantum numbers that take fixed values ($N=1$ and $l=2$) have been omitted from basis kets for clarity. We see that by far the largest contribution to the unphysical state is given by the states in the $J_r=2$ block. This suggests that, as shown in the next section, the unphysical states do not affect the results of quantum scattering calculations on ultracold molecular collisions, which are determined by the lowest J_r states in the TRAM basis.

As shown in the lower panel of Fig. 2, the $N=0$ eigenstates computed in the TRAM basis are nearly identical to the physical hyperfine-Zeeman states of YbF, with the relative deviations not exceeding 0.01%. This is because the different J_r blocks are only coupled by the relatively weak, field-independent spin-rotation and anisotropic hyperfine interactions. This is in contrast to the TAM representation, where the different J blocks are coupled by the external magnetic field, causing the appearance of distinct unphysical Zeeman states in all N manifolds even in the absence of hyperfine structure [33,34,36].

The $N=1$ manifold has more unphysical states especially at smaller magnetic fields, where the couplings between the different J_r blocks are larger than the Zeeman interaction.

Even for these states, the relative deviation between the physical and unphysical energies does not exceed 0.07%. The largest deviation occurs for the state closest to state $|9\rangle$ marked by an arrow in Fig. 2. In addition, the density of unphysical states in the TRAM basis is significantly lower than in the TAM representation, where *most* of the $N = 1$ states are unphysical [36]. The lower density of unphysical states represents an advantage of the TRAM basis over the TAM basis [33,34,36].

B. Ultracold atom-molecule collision dynamics in the TRAM basis

To gauge the accuracy and computational efficiency of our TRAM basis, we have developed a scattering code implementing CC equations in this basis for $^2\Sigma$ molecule–^{1}S atom collisions as described in Sec. II A. The CC equations are parametrized by the matrix elements of the intramolecular Hamiltonian of YbF and of the He-YbF interaction potential as described in Ref. [54] and in Sec. II A.

For comparison with previous quantum scattering calculations on He + YbF [54] using the fully uncoupled basis, we used the same cutoff parameter for the rotational states $N^{\max} = 8$, but varied the cutoff parameter $J_r^{\max} = 2$ and 3. The CC equations are integrated using the log-derivative propagator [94,95] on a grid of R extending from 3.84 to 80 a_0 with the grid step of 0.04 a_0. The following values of atomic and molecular masses were used in CC calculations (in atomic mass units): $m_{\rm He} = 3.016\,03$ and $m_{\rm YbF} = 192.937\,265\,2$. At the end of the propagation, the log-derivative matrix is transformed to the basis, in which the asymptotic Hamiltonian is diagonal, and then matched to the asymptotic boundary conditions to produce the reactance (K) and scattering (S) matrices, from which the integral cross sections are obtained using the standard expressions

$$\sigma_{\gamma\to\gamma'} = \frac{\pi}{k_\gamma^2}\sum_M\sum_{l,l'}\left|\delta_{\gamma\gamma'}\delta_{ll'} - S^M_{\gamma l,\gamma' l'}\right|^2, \qquad (30)$$

where the index $\gamma = 1, 2, \ldots$ labels the eigenvalues of the asymptotic Hamiltonian in the order of increasing energy (see Fig. 2). The unphysical states are assigned to the physical eigenstates that are closest in energy. The calculated cross sections are converged to $\leqslant 5\%$.

Figure 3 compares state-to-state cross sections for ultracold He + YbF collisions calculated using the TRAM basis set with reference calculations [54]. The cross sections calculated using these completely unrelated bases are in excellent agreement with each other across the entire range of magnetic fields, validating the accuracy of our TRAM calculations. Taking the $|4\rangle \to |1\rangle$ transition as an example, the relative differences between the TRAM cross sections and the reference data do not exceed 0.1% at magnetic fields below 0.04 T (for $J_r^{\max} = 3$). The deviations increase to a few percent at higher magnetic fields, most likely due to incomplete convergence of the reference results [54].

Using a minimal basis set including the three lowest J_r blocks ($J_r^{\max} = 2$) is sufficient for magnetic fields below 0.1 T. Above this field value, a higher value of $J_r^{\max} = 3$ is required for the hyperfine transitions $|4\rangle \to |1\rangle$ and $|4\rangle \to |2\rangle$. As shown in Fig. 2, the final states $|1\rangle$ and $|2\rangle$ are low-field seeking, whereas the initial state $|4\rangle$ is high-field seeking. Thus, the transitions $|4\rangle \to |1\rangle$ and $|4\rangle \to |2\rangle$ release an increasing amount of energy with increasing magnetic field, leading to the population of higher partial wave states in the outgoing collision channel, and necessitating the use of larger $J_r^{\max}$.

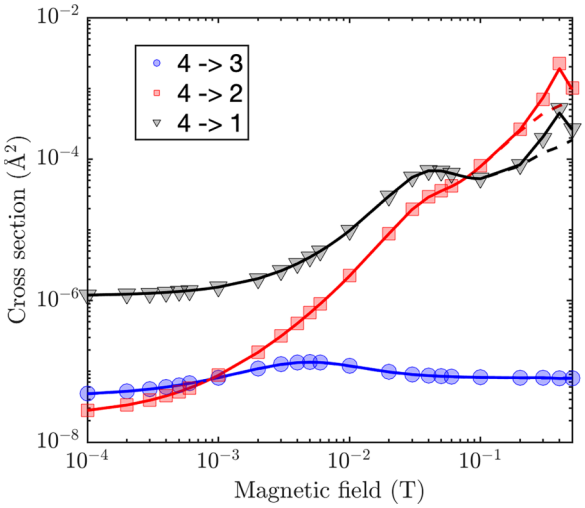

FIG. 3. Magnetic-field dependence of the integral cross sections for ultracold He + YbF collisions with YbF molecules initially in the fully spin-polarized state $|4\rangle$ (see Fig. 2) and the final states $|3\rangle$ (circles), $|2\rangle$ (squares), and $|1\rangle$ (triangles). Solid lines, TRAM calculations with $J_r^{\max} = 3$; dashed lines, TRAM calculations with $J_r^{\max} = 2$; symbols, benchmark calculations using the fully uncoupled basis [54]. The collision energy is 1 mK.

The reference calculations employed the fully uncoupled basis set with $N^{\max} = 8$ and $l^{\max} = 9$ [54], leading to 2262 coupled channels for the total angular momentum projection $M = 0$. By comparison, the TRAM basis with the same num-

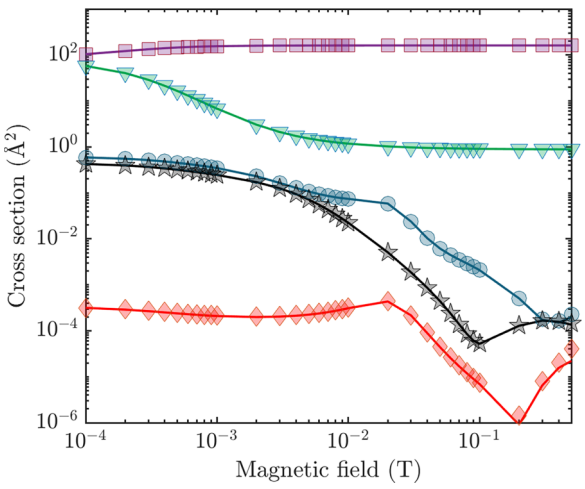

FIG. 4. Magnetic-field dependence of the integral cross sections for ultracold He + YbF collisions with YbF molecules initially in the rotationally excited state $|16\rangle$ and the final Zeeman states $|8\rangle$ (circles), $|4\rangle$ (squares), $|3\rangle$ (triangles), $|2\rangle$ (diamonds), and $|1\rangle$ (stars) (see Fig. 2). TRAM calculations with $J_r^{\max} = 3$ (solid lines) are compared with benchmark calculations (symbols) using the fully uncoupled basis [54]. The collision energy is 1 mK.

ber of rotational states and $J_r^{\max} = 2$ includes 274 channels for the same value of M, a reduction in the number of coupled channels by the factor of 8.2. The computational cost of solving CC equations scales as N^3 with the number of channels. Thus, using the TRAM basis leads to a 550-fold increase in computational efficiency compared to the fully uncoupled basis used in the previous calculations [54].

Figure 4 shows the inelastic cross sections for YbF molecules initially in the highest low-field seeking hyperfine-Zeeman sublevel of the $N = 1$ rotational state (state $|16\rangle$ in Fig. 2). Inelastic collisions with He atoms can either conserve or change the rotational state of YbF. All the state-to-state cross sections calculated using the TRAM basis are in excellent agreement with the benchmark values, demonstrating the ability of the TRAM basis set to accurately describe ultracold collisions of rotationally excited molecules. The unphysical states shown in the upper panel of Fig. 2 do not affect the results of CC calculations for reasons discussed in Sec. III A.

IV. SUMMARY AND OUTLOOK

Hyperfine interactions play an essential role in ultracold atomic and molecular collisions, being largely responsible, for, e.g., positions and widths of magnetic Feshbach resonances in ultracold collisions of alkali-metal atoms [41]. Quantum scattering calculations must therefore account for hyperfine structure in order to provide a realistic picture of ultracold atom-molecule and molecule-molecule collision dynamics in the presence of external electromagnetic fields.

While it is possible to include the hyperfine structure directly in the TAM representation, this approach is hindered by two difficulties. First, unphysical states show up in the spectrum of threshold energy levels in the presence of external fields [33,34,36]. Even though these states do not affect the dynamics of ultracold collisions, and they can be eliminated by augmenting the basis set [36], they can pose a challenge for bound-state calculations [36,96]. Second, constructing the TAM basis functions requires multiple angular momentum coupling operations to form the eigenstates of $\hat{J}^2$ and $\hat{J}_Z$. This leads to complicated expressions for the matrix elements of the interaction potential and/or the centrifugal kinetic energy [33,35], which can be challenging to implement in actual numerical calculations.

Here, we have explored an alternative basis set composed of products of eigenfunctions of the TRAM of the collision complex J_r and the spin basis functions of its constituent atoms and molecules. In the absence of spin-rotation interactions, J_r is conserved and the scattering problem can be rigorously block diagonalized and solved separately for each value J_r even in the presence of external magnetic field and isotropic hyperfine interactions. This makes the TRAM basis particularly promising for molecules, whose collision dynamics is dominated by the isotropic hyperfine and Zeeman interactions (in addition to the electrostatic interaction potential). By contrast, the scattering Hamiltonian in the TAM representation [33,34] is not block diagonalizable in the presence of external magnetic fields.

In addition, the matrix elements of the Hamiltonian in the TRAM basis are simple to evaluate and program, and the unphysical states are eliminated for $N = 0$. Even though such states are still present for $N \geqslant 1$, their density is significantly reduced compared to that in the TAM representation [36]. This is because the unphysical states in the TRAM basis arise due to the matrix elements of the anisotropic hyperfine and spin-rotation interactions that are off diagonal in J_r and independent of magnetic field. These matrix elements are small compared to those of the Zeeman interaction at moderate to strong magnetic fields (above $\simeq 100$ G). As a result, most of the eigenvalues of the asymptotic Hamiltonian in the TRAM basis are close to the physical hyperfine-Zeeman states, and thus the density of unphysical states is low. By contrast, in the TAM representation, the matrix elements off diagonal in J responsible for the unphysical states are due to the Zeeman interaction [33], which is generally much stronger, and causes a substantially higher density of unphysical states, especially for $N \geqslant 1$ [36].

We formulate the quantum scattering problem in the TRAM basis for collisions of $^2\Sigma$ molecules with ^{1}S atoms (Sec. IIA) and with ^{2}S atoms (Sec. IIB). The generalized spin-rotation interactions, which couple the different values of J_r, include the electron-spin–rotation and anisotropic hyperfine interactions, as well as the intermolecular magnetic dipole-dipole interaction (see Fig. 1). When these interactions are non-negligible, they can be incorporated in a straightforward manner by including several J_r states in the TRAM basis as discussed in Sec. II. This is demonstrated by our CC calculations on ultracold s-wave He + YbF($^2\Sigma$) collisions in the regime where the electron-spin–rotation and anisotropic hyperfine interactions in YbF are non-negligible (see Sec. III). With the three lowest J_r blocks in the basis, we observe excellent agreement of state-to-state scattering cross sections with prior calculations [54] using eight times fewer TRAM basis functions, leading to a computational gain of about three orders of magnitude over the fully uncoupled basis [54]. Even larger gains are expected for ultracold collisions of $^2\Sigma$ molecules with ^{2}S atoms considered in Sec. IIB.

Despite mounting experimental studies of Feshbach resonances in ultracold atom-molecule [45,46,48,65,97,98] and molecule-molecule [51] collisions, rigorous quantum dynamics calculations on such collisions are currently beyond reach. As discussed above, this is partly due to the difficulties associated with including the effects of atomic and molecular hyperfine structure and/or external fields. It is our hope that the computationally efficient and easy-to-implement TRAM representation will facilitate such calculations in the near future. It would also be interesting to extend the TRAM approach to ultracold molecule-molecule collisions and to other types of CC basis sets, such as those defined in the body-fixed coordinate frame [13,33,99].

ACKNOWLEDGMENTS

We thank Dr. Masato Morita for verifying Eq. (28). The work at the University of Nevada, Reno was supported by the NSF through the CAREER program (Grant No. PHY-2045681). The work at JILA was supported by the NSF (Grant No. PHY-2012125) and by NASA Jet Propulsion Laboratory (Grant No. 1502690).

APPENDIX A: MATRIX ELEMENTS OF THE ELECTRON-SPIN–ROTATION INTERACTION IN THE TRAM BASIS

Here, we derive the matrix elements of the intramolecular electron-spin–rotation interaction in the TRAM basis. Expanding the spin-rotation interaction in rank-1 spherical tensor operators $\hat{N}^{(1)}_{\pm 1} = \mp\frac{1}{\sqrt{2}}\hat{N}_{\pm} = \mp\frac{1}{\sqrt{2}}(\hat{N}_X \pm \hat{N}_Y)$ and $\hat{N}^{(1)}_0 = \hat{N}_Z$ (and similarly for $\hat{S}^{(1)}_p$) [84],

$$\gamma_{\rm SR}\hat{\mathbf{N}}\cdot\hat{\mathbf{S}} = \gamma_{\rm SR}\sum_{p=-1}^{1}(-1)^q \hat{N}^{(1)}_p \hat{S}^{(1)}_{-p}, \tag{A1}$$

and using the direct-product structure of the TRAM basis gives (omitting the basis functions $|IM_I\rangle$ for clarity)

$$\langle (Nl)J_rM_r|\langle SM_S|\gamma_{\rm SR}\hat{\mathbf{N}}\cdot\hat{\mathbf{S}}|(N'l')J'_rM'_r\rangle|SM'_S\rangle = \gamma_{\rm SR}\sum_{p=-1}^{1}(-1)^q\langle (Nl)J_rM_r|\hat{N}^{(1)}_p|(N'l')J'_rM'_r\rangle\langle SM_S|\hat{S}^{(1)}_{-p}|SM'_S\rangle. \tag{A2}$$

Applying the Wigner-Eckart theorem to the rotational matrix element on the right-hand side,

$$\langle (Nl)J_rM_r|\hat{N}^{(1)}_p|(N'l')J'_rM'_r\rangle = (-1)^{J_r-M_r}\begin{pmatrix} J_r & 1 & J'_r \\ -M_r & p & M'_r\end{pmatrix}\langle (Nl)J_r||\hat{N}^{(1)}||(N'l')J'_r\rangle, \tag{A3}$$

and simplifying the resulting double-bar matrix element [84] we get

$$\begin{aligned}\langle (Nl)J_rM_r|\hat{N}^{(1)}_p|(N'l')J'_rM'_r\rangle =& (-1)^{J_r-M_r}\begin{pmatrix} J_r & 1 & J'_r \\ -M_r & p & M'_r\end{pmatrix}\delta_{ll'}(-1)^{N+l+J'_r+1}[(2J_r+1)(2J'_r+1)]^{1/2}\\ &\times\begin{Bmatrix} N & J_r & l \\ J'_r & N & 1\end{Bmatrix}[(2N+1)N(N+1)]^{1/2}\delta_{NN'}.\end{aligned} \tag{A4}$$

Using

$$\langle SM_S|\hat{S}^{(1)}_{-p}|SM'_S\rangle = (-1)^{S-M_S}\begin{pmatrix} S & 1 & S \\ -M_S & -p & M'_S\end{pmatrix}[(2S+1)S(S+1)]^{1/2} \tag{A5}$$

in combination with Eqs. (A4) and (A2), we obtain Eq. (13) of the main text.

APPENDIX B: MATRIX ELEMENTS OF THE ANISOTROPIC HYPERFINE INTERACTION IN THE TRAM BASIS

The anisotropic hyperfine interaction given by the last term in Eq. (5) is composed of three tensor operators, which depend on the rotational, electron-spin, and nuclear-spin variables:

$$\hat{H}^{\rm AHF}_{\rm mol} = \frac{c\sqrt{6}}{3}\left(\frac{4\pi}{5}\right)^{1/2}\sum_{q=-2}^{2}(-1)^q Y_{2-q}(\theta_r,\phi_r)[\hat{\mathbf{I}}\otimes\hat{\mathbf{S}}]^{(2)}_q. \tag{B1}$$

Taking the matrix elements of this expression in the TRAM basis, we find

$$\begin{aligned}\langle (Nl)J_rM_r|\langle SM_S|\langle IM_I|\hat{H}^{\rm AHF}_{\rm mol}|(N'l')J'_rM'_r\rangle|SM'_S\rangle|IM'_I\rangle =& \frac{c\sqrt{6}}{3}\left(\frac{4\pi}{5}\right)^{1/2}\sum_{q=-2}^{2}(-1)^q\langle (Nl)J_rM_r|Y_{2-q}|(N'l')J'_rM'_r\rangle\\ &\times\langle SM_S|\langle IM_I|[\hat{\mathbf{I}}\otimes\hat{\mathbf{S}}]^{(2)}_q|SM'_S\rangle|IM'_I\rangle.\end{aligned} \tag{B2}$$

The first matrix element on the right-hand side can be evaluated using the Wigner-Eckart theorem [84]

$$\langle (Nl)J_rM_r|Y_{2-q}|(N'l')J'_rM'_r\rangle = (-1)^{J_r-M_r}\begin{pmatrix} J_r & 2 & J'_r \\ -M_r & -q & M'_r\end{pmatrix}\langle (Nl)J_r||Y^{(2)}||(N'l')J'_r\rangle \tag{B3}$$

with the double-bar matrix element given by [84]

$$\langle (Nl)J_r||Y^{(2)}||(N'l')J'_r\rangle = \delta_{ll'}(-1)^{l+J'_r}[(2J_r+1)(2J'_r+1)]^{1/2}\begin{Bmatrix} N & J_r & l \\ J'_r & N' & 2\end{Bmatrix}\left(\frac{5}{4\pi}\right)^{1/2}[(2N+1)(2N'+1)]^{1/2}\begin{pmatrix} N & 2 & N' \\ 0 & 0 & 0\end{pmatrix}. \tag{B4}$$

It remains to consider the spin matrix element

$$\langle SM_S|\langle IM_I|[\hat{\mathbf{I}}\otimes\hat{\mathbf{S}}]^{(2)}_q|SM'_S\rangle|IM'_I\rangle = \sum_{q_I,q_S}(-1)^q\sqrt{5}\begin{pmatrix} 1 & 1 & 2 \\ q_I & q_S & -q\end{pmatrix}\langle IM_I|\hat{I}^{(1)}_{q_I}|IM'_I\rangle\langle SM_S|\hat{S}^{(1)}_{q_S}|SM'_S\rangle \tag{B5}$$

where we have used the definition of the tensor product of two spherical tensor operators [84]. Using once again the Wigner-Eckart theorem

$$\langle IM_I|\hat{I}^{(1)}_{q_I}|IM'_I\rangle = (-1)^{I-M_I}\begin{pmatrix} I & 1 & I \\ -M_I & q_I & M'_I \end{pmatrix}[(2I+1)I(I+1)]^{1/2} \tag{B6}$$

and the corresponding expression for the matrix elements of $\hat{S}^{(1)}_{q_S}$, we obtain

$$\langle SM_S|\langle IM_I|[\hat{\mathbf{I}}\otimes\hat{\mathbf{S}}]^{(2)}_q|SM'_S\rangle|IM'_I\rangle = \sum_{q_I,q_S}(-1)^q\sqrt{5}\begin{pmatrix} 1 & 1 & 2 \\ q_I & q_S & -q \end{pmatrix}(-1)^{I-M_I+S-M_S}\begin{pmatrix} I & 1 & I \\ -M_I & q_I & M'_I \end{pmatrix}$$
$$\times\,[(2I+1)I(I+1)(2S+1)S(S+1)]^{1/2}\begin{pmatrix} S & 1 & S \\ -M_S & q_S & M'_S \end{pmatrix}. \tag{B7}$$

This expression, combined with Eqs. (B4) and (B2), gives Eq. (14) of the main text.

APPENDIX C: MATRIX ELEMENTS OF THE MAGNETIC DIPOLE-DIPOLE INTERACTION IN THE TRAM BASIS

Finally, we consider the matrix elements of the magnetic dipole-dipole interaction, which does not affect the nuclear-spin degrees of freedom, and is thus diagonal in M_I and M_{I_a}. Omitting the nuclear-spin basis functions and using the shorthand notation $|M_S M_{S_a}\rangle$ for the electron-spin basis functions $|SM_S\rangle|S_a M_{S_a}\rangle$ the matrix elements take the form

$$\langle (Nl)J_rM_r|\langle M_SM_{S_a}|\hat{V}_{\rm MDD}|(N'l')J'_rM'_r\rangle|M'_SM'_{S_a}\rangle = -\sqrt{\frac{24\pi}{5}}\frac{\alpha^2}{R^3}\sum_q(-1)^q\langle (Nl)J_rM_r|Y_{2,-q}(\hat{R})|(N'l')J'_rM'_r\rangle$$
$$\times\,\langle M_SM_{S_a}|[\hat{\mathbf{S}}\otimes\hat{\mathbf{S}}_a]^{(2)}_q|M'_SM'_{S_a}\rangle. \tag{C1}$$

The Wigner-Eckart theorem allows us to factorize the orbital matrix element involving the spherical harmonics $Y_{2,-q}(\hat{R})$ as

$$\langle (Nl)J_rM_r|Y_{2,-q}(\hat{R})|(N'l')J'_rM'_r\rangle = (-1)^{J_r-M_r}\begin{pmatrix} J_r & 2 & J'_r \\ -M_r & -q & M'_r \end{pmatrix}\langle (Nl)J_r||\hat{Y}^{(2)}||(N'l')J'_r\rangle. \tag{C2}$$

Evaluating the double-bar matrix element [84] we obtain

$$\langle (Nl)J_rM_r|Y_{2,-q}(\hat{R})|(N'l')J'_rM'_r\rangle = (-1)^{J_r-M_r}\begin{pmatrix} J_r & 2 & J'_r \\ -M_r & -q & M'_r \end{pmatrix}\delta_{NN'}(-1)^{N+l'+J_r}[(2J_r+1)(2J'_r+1)]^{1/2}\begin{Bmatrix} l & J_r & N \\ J'_r & l' & 2 \end{Bmatrix}$$
$$\times\,(-1)^l[(2l+1)(2l'+1)]^{1/2}\sqrt{\frac{5}{4\pi}}\begin{pmatrix} l & 2 & l' \\ 0 & 0 & 0 \end{pmatrix}. \tag{C3}$$

The spin matrix element in Eq. (C1) can be evaluated as described in Appendix B:

$$\langle M_SM_{S_a}|[\hat{\mathbf{S}}\otimes\hat{\mathbf{S}}_a]^{(2)}_q|M'_SM'_{S_a}\rangle = \sum_{q_S,q_{S_a}}(-1)^q\sqrt{5}\begin{pmatrix} 1 & 1 & 2 \\ q_S & q_{S_a} & -q \end{pmatrix}(-1)^{S-M_S+S_a-M_{S_a}}\begin{pmatrix} S & 1 & S \\ -M_S & q_S & M'_S \end{pmatrix}$$
$$\times\,[(2S+1)S(S+1)]^{1/2}[(2S_a+1)S_a(S_a+1)]^{1/2}\begin{pmatrix} S_a & 1 & S_a \\ -M_{S_a} & q_{S_a} & M'_{S_a} \end{pmatrix}. \tag{C4}$$

Combining this result with Eq. (C3) and setting $q_S = M_S - M'_S$, $q_{S_a} = M_{S_a} - M'_{S_a}$, and $-q = M_r - M'_r$, we obtain Eq. (28) of the main text.

[1] L. D. Carr, D. DeMille, R. V. Krems, and J. Ye, Cold and ultracold molecules: Science, technology and applications, New J. Phys. **11**, 055049 (2009).

[2] J. L. Bohn, A. M. Rey, and J. Ye, Cold molecules: Progress in quantum engineering of chemistry and quantum matter, Science **357**, 1002 (2017).

[3] S. F. Yelin, K. Kirby, and R. Côté, Schemes for robust quantum computation with polar molecules, Phys. Rev. A **74**, 050301(R) (2006).

[4] A. V. Gorshkov, S. R. Manmana, G. Chen, E. Demler, M. D. Lukin, and A. M. Rey, Quantum magnetism with polar alkali-metal dimers, Phys. Rev. A **84**, 033619 (2011).

[5] V. V. Albert, J. P. Covey, and J. Preskill, Robust encoding of a qubit in a molecule, Phys. Rev. X **10**, 031050 (2020).

[6] R. V. Krems, Cold controlled chemistry, Phys. Chem. Chem. Phys. **10**, 4079 (2008).

[7] N. Balakrishnan, Perspective: Ultracold molecules and the dawn of cold controlled chemistry, J. Chem. Phys. **145**, 150901 (2016).

[8] R. V. Krems, *Molecules in Electromagnetic Fields* (Wiley, New York, 2019).

[9] Y. Liu and K.-K. Ni, Bimolecular chemistry in the ultracold regime, Annu. Rev. Phys. Chem. **73**, 73 (2022).

[10] M. Mayle, G. Quéméner, B. P. Ruzic, and J. L. Bohn, Scattering of ultracold molecules in the highly resonant regime, Phys. Rev. A **87**, 012709 (2013).

[11] Y. Liu, M.-G. Hu, M. A. Nichols, D. D. Grimes, T. Karman, H. Guo, and K.-K. Ni, Photo-excitation of long-lived transient intermediates in ultracold reactions, Nat. Phys. **16**, 1132 (2020).

[12] T. V. Tscherbul, J. Kłos, and A. A. Buchachenko, Ultracold spin-polarized mixtures of $^2\Sigma$ molecules with S-state atoms: Collisional stability and implications for sympathetic cooling, Phys. Rev. A **84**, 040701(R) (2011).

[13] M. Morita, M. B. Kosicki, P. S. Żuchowski, and T. V. Tscherbul, Atom-molecule collisions, spin relaxation, and sympathetic cooling in an ultracold spin-polarized $Rb(^2S) - SrF(^2\Sigma^+)$ mixture, Phys. Rev. A **98**, 042702 (2018).

[14] M. Morita, J. Kłos, A. A. Buchachenko, and T. V. Tscherbul, Cold collisions of heavy $^2\Sigma$ molecules with alkali-metal atoms in a magnetic field: Ab initio analysis and prospects for sympathetic cooling of $SrOH(^2\Sigma^+)$ by $Li(^2S)$, Phys. Rev. A **95**, 063421 (2017).

[15] M. Child, *Molecular Collision Theory* (Wiley, New York, 1974).

[16] S. C. Althorpe and D. C. Clary, Quantum scattering calculations on chemical reactions, Annu. Rev. Phys. Chem. **54**, 493 (2003).

[17] R. V. Krems, A. Dalgarno, N. Balakrishnan, and G. C. Groenenboom, Spin-flipping transitions in $^2\Sigma$ molecules induced by collisions with structureless atoms, Phys. Rev. A **67**, 060703(R) (2003).

[18] N. Balakrishnan, G. C. Groenenboom, R. V. Krems, and A. Dalgarno, The He-$CaH(^2\Sigma^+)$ interaction. II. Collisions at cold and ultracold temperatures, J. Chem. Phys. **118**, 7386 (2003).

[19] W. C. Campbell, T. V. Tscherbul, H.-I. Lu, E. Tsikata, R. V. Krems, and J. M. Doyle, Mechanism of collisional spin relaxation in $^3\Sigma$ molecules, Phys. Rev. Lett. **102**, 013003 (2009).

[20] M. T. Hummon, T. V. Tscherbul, J. Kłos, H.-I. Lu, E. Tsikata, W. C. Campbell, A. Dalgarno, and J. M. Doyle, Cold N + NH collisions in a magnetic trap, Phys. Rev. Lett. **106**, 053201 (2011).

[21] S. Chefdeville, Y. Kalugina, S. Y. T. van de Meerakker, C. Naulin, F. Lique, and M. Costes, Observation of partial wave resonances in low-energy O_2-H_2 inelastic collisions, Science **341**, 1094 (2013).

[22] S. N. Vogels, J. Onvlee, S. Chefdeville, A. van der Avoird, G. C. Groenenboom, and S. Y. T. van de Meerakker, Imaging resonances in low-energy NO-He inelastic collisions, Science **350**, 787 (2015).

[23] A. Bergeat, J. Onvlee, C. Naulin, A. van der Avoird, and M. Costes, Quantum dynamical resonances in low-energy $CO(j = 0)$ + He inelastic collisions, Nat. Chem. **7**, 349 (2015).

[24] A. Klein, Y. Shagam, W. Skomorowski, P. S. Żuchowski, M. Pawlak, L. M. C. Janssen, N. Moiseyev, S. Y. T. van de Meerakker, A. van der Avoird, C. P. Koch, and E. Narevicius, Directly probing anisotropy in atom–molecule collisions through quantum scattering resonances, Nat. Phys. **13**, 35 (2017).

[25] S. N. Vogels, T. Karman, J. Kłos, M. Besemer, J. Onvlee, A. van der Avoird, G. C. Groenenboom, and S. Y. T. van de Meerakker, Scattering resonances in bimolecular collisions between NO radicals and H_2 challenge the theoretical gold standard, Nat. Chem. **10**, 435 (2018).

[26] T. de Jongh, M. Besemer, Q. Shuai, T. Karman, A. van der Avoird, G. C. Groenenboom, and S. Y. T. van de Meerakker, Imaging the onset of the resonance regime in low-energy NO-He collisions, Science **368**, 626 (2020).

[27] M. Morita, R. V. Krems, and T. V. Tscherbul, Universal probability distributions of scattering observables in ultracold molecular collisions, Phys. Rev. Lett. **123**, 013401 (2019).

[28] T. V. Tscherbul, Y. V. Suleimanov, V. Aquilanti, and R. V. Krems, Magnetic field modification of ultracold molecule–molecule collisions, New J. Phys. **11**, 055021 (2009).

[29] T. V. Tscherbul and R. V. Krems, Tuning bimolecular chemical reactions by electric fields, Phys. Rev. Lett. **115**, 023201 (2015).

[30] M. Morita, J. Kłos, and T. V. Tscherbul, Full-dimensional quantum scattering calculations on ultracold atom-molecule collisions in magnetic fields: The role of molecular vibrations, Phys. Rev. Res. **2**, 043294 (2020).

[31] D. G. Truhlar, Long-standing themes in computational chemical dynamics, Comput. Phys. Commun. **84**, 78 (1994).

[32] A. M. Arthurs and A. Dalgarno, The theory of scattering by a rigid rotator, Proc. R. Soc. A **256**, 540 (1960).

[33] T. V. Tscherbul and A. Dalgarno, Quantum theory of molecular collisions in a magnetic field: Efficient calculations based on the total angular momentum representation, J. Chem. Phys. **133**, 184104 (2010).

[34] T. V. Tscherbul, Total-angular-momentum representation for atom-molecule collisions in electric fields, Phys. Rev. A **85**, 052710 (2012).

[35] Y. V. Suleimanov, T. V. Tscherbul, and R. V. Krems, Efficient method for quantum calculations of molecule-molecule scattering properties in a magnetic field, J. Chem. Phys. **137**, 024103 (2012).

[36] S. Koyu, R. Hermsmeier, and T. V. Tscherbul, Total angular momentum representation for state-to-state quantum scattering of cold molecules in a magnetic field, J. Chem. Phys. **156**, 034112 (2022).

[37] J. Brown and A. Carrington, *Rotational Spectroscopy of Diatomic Molecules* (Cambridge University, New York, 2003).

[38] J. Aldegunde, B. A. Rivington, P. S. Żuchowski, and J. M. Hutson, Hyperfine energy levels of alkali-metal dimers: Ground-state polar molecules in electric and magnetic fields, Phys. Rev. A **78**, 033434 (2008).

[39] A. L. Collopy, M. T. Hummon, M. Yeo, B. Yan, and J. Ye, Prospects for a narrow line MOT in YO, New J. Phys. **17**, 055008 (2015).

[40] J. J. Burau, P. Aggarwal, K. Mehling, and J. Ye, Blue-detuned magneto-optical trap of molecules, Phys. Rev. Lett. **130**, 193401 (2023).

[41] C. Chin, R. Grimm, P. Julienne, and E. Tiesinga, Feshbach resonances in ultracold gases, Rev. Mod. Phys. **82**, 1225 (2010).

[42] M. Mayle, B. P. Ruzic, and J. L. Bohn, Statistical aspects of ultracold resonant scattering, Phys. Rev. A **85**, 062712 (2012).

[43] M.-G. Hu, Y. Liu, M. A. Nichols, L. Zhu, G. Quéméner, O. Dulieu, and K.-K. Ni, Nuclear spin conservation enables state-to-state control of ultracold molecular reactions, Nat. Chem. **13**, 435 (2021).

[44] G. Quéméner, M.-G. Hu, Y. Liu, M. A. Nichols, L. Zhu, and K.-K. Ni, Model for nuclear spin product-state distributions of ultracold chemical reactions in magnetic fields, Phys. Rev. A **104**, 052817 (2021).

[45] H. Yang, D.-C. Zhang, L. Liu, Y.-X. Liu, J. Nan, B. Zhao, and J.-W. Pan, Observation of magnetically tunable Feshbach

resonances in ultracold ^{23}Na ^{40}K + ^{40}K collisions, Science **363**, 261 (2019).

[46] Z. Su, H. Yang, J. Cao, X.-Y. Wang, J. Rui, B. Zhao, and J.-W. Pan, Resonant control of elastic collisions between ^{23}Na ^{40}K molecules and ^{40}K atoms, Phys. Rev. Lett. **129**, 033401 (2022).

[47] M. A. Nichols, Y.-X. Liu, L. Zhu, M.-G. Hu, Y. Liu, and K.-K. Ni, Detection of long-lived complexes in ultracold atom-molecule collisions, Phys. Rev. X **12**, 011049 (2022).

[48] J. J. Park, H. Son, Y.-K. Lu, T. Karman, M. Gronowski, M. Tomza, A. O. Jamison, and W. Ketterle, Spectrum of Feshbach resonances in NaLi + Na collisions, Phys. Rev. X **13**, 031018 (2023).

[49] T. Karman, M. Gronowski, M. Tomza, J. J. Park, H. Son, Y.-K. Lu, A. O. Jamison, and W. Ketterle, *Ab initio* calculation of the spectrum of Feshbach resonances in NaLi + Na collisions, Phys. Rev. A **108**, 023309 (2023).

[50] M. G. Hu, Y. Liu, D. D. Grimes, Y. W. Lin, A. H. Gheorghe, R. Vexiau, N. Bouloufa-Maafa, O. Dulieu, T. Rosenband, and K. K. Ni, Direct observation of bimolecular reactions of ultracold KRb molecules, Science **366**, 1111 (2019).

[51] J. J. Park, Y.-K. Lu, A. O. Jamison, T. V. Tscherbul, and W. Ketterle, A Feshbach resonance in collisions between triplet ground-state molecules, Nature (London) **614**, 54 (2023).

[52] A. Volpi and J. L. Bohn, Magnetic-field effects in ultracold molecular collisions, Phys. Rev. A **65**, 052712 (2002).

[53] R. V. Krems and A. Dalgarno, Quantum-mechanical theory of atom-molecule and molecular collisions in a magnetic field: Spin depolarization, J. Chem. Phys. **120**, 2296 (2004).

[54] T. V. Tscherbul, J. Kłos, L. Rajchel, and R. V. Krems, Fine and hyperfine interactions in cold YbF-He collisions in electromagnetic fields, Phys. Rev. A **75**, 033416 (2007).

[55] M. Lara, J. L. Bohn, D. Potter, P. Soldán, and J. M. Hutson, Ultracold Rb-OH collisions and prospects for sympathetic cooling, Phys. Rev. Lett. **97**, 183201 (2006).

[56] M. Lara, J. L. Bohn, D. E. Potter, P. Soldán, and J. M. Hutson, Cold collisions between OH and Rb: The field-free case, Phys. Rev. A **75**, 012704 (2007).

[57] M. L. González-Martínez and J. M. Hutson, Effect of hyperfine interactions on ultracold molecular collisions: NH($^3\Sigma^-$) with Mg(^{1}S) in magnetic fields, Phys. Rev. A **84**, 052706 (2011).

[58] R. Hermsmeier, X. Xing, and T. V. Tscherbul, Nuclear spin relaxation in cold atom–molecule collisions, J. Phys. Chem. A **127**, 4511 (2023).

[59] A. O. G. Wallis and R. V. Krems, Magnetic Feshbach resonances in collisions of nonmagnetic closed-shell $^1\Sigma$ molecules, Phys. Rev. A **89**, 032716 (2014).

[60] T. V. Tscherbul and J. Kłos, Magnetic tuning of ultracold barrierless chemical reactions, Phys. Rev. Res. **2**, 013117 (2020).

[61] R. Hermsmeier, J. Kłos, S. Kotochigova, and T. V. Tscherbul, Quantum spin state selectivity and magnetic tuning of ultracold chemical reactions of triplet alkali-metal dimers with alkali-metal atoms, Phys. Rev. Lett. **127**, 103402 (2021).

[62] N. Akerman, M. Karpov, Y. Segev, N. Bibelnik, J. Narevicius, and E. Narevicius, Trapping of molecular oxygen together with lithium atoms, Phys. Rev. Lett. **119**, 073204 (2017).

[63] S. Jurgilas, A. Chakraborty, C. J. H. Rich, L. Caldwell, H. J. Williams, N. J. Fitch, B. E. Sauer, M. D. Frye, J. M. Hutson, and M. R. Tarbutt, Collisions between ultracold molecules and atoms in a magnetic trap, Phys. Rev. Lett. **126**, 153401 (2021).

[64] H. Son, J. J. Park, W. Ketterle, and A. O. Jamison, Collisional cooling of ultracold molecules, Nature (London) **580**, 197 (2020).

[65] H. Son, J. J. Park, Y.-K. Lu, A. O. Jamison, T. Karman, and W. Ketterle, Control of reactive collisions by quantum interference, Science **375**, 1006 (2022).

[66] B. K. Kendrick, H. Li, M. Li, S. Kotochigova, J. F. E. Croft, and N. Balakrishnan, Non-adiabatic quantum interference in the ultracold Li + LiNa → Li_2+ Na reaction, Phys. Chem. Chem. Phys. **23**, 5096 (2021).

[67] M. Morita, B. K. Kendrick, J. Kłos, S. Kotochigova, P. Brumer, and T. V. Tscherbul, Signatures of non-universal quantum dynamics of ultracold chemical reactions of polar alkali dimer molecules with alkali metal atoms: Li(^{2}S) + NaLi($a^3\Sigma^+$) → Na(^{2}S) + Li_2($a^3\Sigma_u^+$), J. Phys. Chem. Lett. **14**, 3413 (2023).

[68] A. Simoni and J. M. Launay, Ultracold atom-molecule collisions with hyperfine coupling, Laser Phys. **16**, 707 (2006).

[69] R. Chapurin, X. Xie, M. J. Van de Graaff, J. S. Popowski, J. P. D'Incao, P. S. Julienne, J. Ye, and E. A. Cornell, Precision test of the limits to universality in few-body physics, Phys. Rev. Lett. **123**, 233402 (2019).

[70] X. Xie, M. J. Van de Graaff, R. Chapurin, M. D. Frye, J. M. Hutson, J. P. D'Incao, P. S. Julienne, J. Ye, and E. A. Cornell, Observation of Efimov universality across a nonuniversal Feshbach resonance in ^{39}K, Phys. Rev. Lett. **125**, 243401 (2020).

[71] J. P. D'Incao and P. S. Julienne (unpublished).

[72] J. F. Barry, D. J. McCarron, E. B. Norrgard, M. H. Steinecker, and D. DeMille, Magneto-optical trapping of a diatomic molecule, Nature (London) **512**, 286 (2014).

[73] D. J. McCarron, M. H. Steinecker, Y. Zhu, and D. DeMille, Magnetic trapping of an ultracold gas of polar molecules, Phys. Rev. Lett. **121**, 013202 (2018).

[74] L. Anderegg, B. L. Augenbraun, Y. Bao, S. Burchesky, L. W. Cheuk, W. Ketterle, and J. M. Doyle, Laser cooling of optically trapped molecules, Nat. Phys. **14**, 890 (2018).

[75] J. Lim, J. R. Almond, M. A. Trigatzis, J. A. Devlin, N. J. Fitch, B. E. Sauer, M. R. Tarbutt, and E. A. Hinds, Laser cooled YbF molecules for measuring the electron's electric dipole moment, Phys. Rev. Lett. **120**, 123201 (2018).

[76] T. K. Langin, V. Jorapur, Y. Zhu, Q. Wang, and D. DeMille, Polarization enhanced deep optical dipole trapping of Λ-cooled polar molecules, Phys. Rev. Lett. **127**, 163201 (2021).

[77] T. K. Langin and D. DeMille, Toward improved loading, cooling, and trapping of molecules in magneto-optical traps, New J. Phys. **25**, 043005 (2023).

[78] N. R. Hutzler, H.-I. Lu, and J. M. Doyle, The buffer gas beam: An intense, cold, and slow source for atoms and molecules, Chem. Rev. **112**, 4803 (2012).

[79] T. V. Tscherbul, *Cold Chemistry: Molecular Scattering and Reactivity Near Absolute Zero* (Royal Society of Chemistry, London, 2018), Chap. 6.

[80] S. Truppe, H. J. Williams, M. Hambach, L. Caldwell, N. J. Fitch, E. A. Hinds, B. E. Sauer, and M. R. Tarbutt, Molecules cooled below the doppler limit, Nat. Phys. **13**, 1173 (2017).

[81] L. Anderegg, L. W. Cheuk, Y. Bao, S. Burchesky, W. Ketterle, K.-K. Ni, and J. M. Doyle, An optical tweezer array of ultracold molecules, Science **365**, 1156 (2019).

[82] S. Ding, Y. Wu, I. A. Finneran, J. J. Burau, and J. Ye, Sub-doppler cooling and compressed trapping of YO molecules at μK temperatures, Phys. Rev. X **10**, 021049 (2020).

[83] Y. Wu, J. J. Burau, K. Mehling, J. Ye, and S. Ding, High phase-space density of laser-cooled molecules in an optical lattice, Phys. Rev. Lett. **127**, 263201 (2021).

[84] R. N. Zare, *Angular Momentum* (Wiley, New York, 1988).

[85] W. Lester, Jr., *Dynamics of Molecular Collisions* (Plenum, New York, 1976), Chap. 1.

[86] A. Schweiger and G. Jeschke, *Principles of Pulse Electron Paramagnetic Resonance* (Cambridge University, New York, 2001).

[87] S. Upadhyay, U. Dargyte, V. D. Dergachev, R. P. Prater, S. A. Varganov, T. V. Tscherbul, D. Patterson, and J. D. Weinstein, Spin coherence and optical properties of alkali-metal atoms in solid parahydrogen, Phys. Rev. A **100**, 063419 (2019).

[88] T. V. Tscherbul, P. Zhang, H. R. Sadeghpour, and A. Dalgarno, Collision-induced spin exchange of alkali-metal atoms with ^{3}He: An ab initio study, Phys. Rev. A **79**, 062707 (2009).

[89] T. V. Tscherbul, P. Zhang, H. R. Sadeghpour, and A. Dalgarno, Anisotropic hyperfine interactions limit the efficiency of spin-exchange optical pumping of ^{3}He nuclei, Phys. Rev. Lett. **107**, 023204 (2011).

[90] K. Jachymski, M. Gronowski, and M. Tomza, Collisional losses of ultracold molecules due to intermediate complex formation, Phys. Rev. A **106**, L041301 (2022).

[91] M. Karplus and R. N. Porter, *Atoms and Molecules* (Benjamin, New York, 1970).

[92] L. M. C. Janssen, A. van der Avoird, and G. C. Groenenboom, On the role of the magnetic dipolar interaction in cold and ultracold collisions: Numerical and analytical results for $\mathrm{NH}(^3\Sigma^-) + \mathrm{NH}(^3\Sigma^-)$, Eur. Phys. J. D **65**, 177 (2011).

[93] J. J. Hudson, D. M. Kara, I. J. Smallman, B. E. Sauer, M. R. Tarbutt, and E. A. Hinds, Improved measurement of the shape of the electron, Nature (London) **473**, 493 (2011).

[94] B. R. Johnson, The multichannel log-derivative method for scattering calculations, J. Comput. Phys. **13**, 445 (1973).

[95] D. E. Manolopoulos, An improved log derivative method for inelastic scattering, J. Chem. Phys. **85**, 6425 (1986).

[96] R. Vexiau, J.-M. Launay, and A. Simoni, Quasi-one-dimensional ultracold rigid-rotor collisions: Reactive and non-reactive cases, Phys. Rev. A **100**, 012704 (2019).

[97] X.-Y. Wang, M. D. Frye, Z. Su, J. Cao, L. Liu, D.-C. Zhang, H. Yang, J. M. Hutson, B. Zhao, C.-L. Bai, and J.-W. Pan, Magnetic Feshbach resonances in collisions of ^{23}Na ^{40}K with ^{40}K, New J. Phys. **23**, 115010 (2021).

[98] H. Yang, J. Cao, Z. Su, J. Rui, B. Zhao, and J.-W. Pan, Creation of an ultracold gas of triatomic molecules from an atom-diatomic molecule mixture, Science **378**, 1009 (2022).

[99] M. Morita and T. V. Tscherbul, Restricted basis set coupled-channel calculations on atom-molecule collisions in magnetic fields, J. Chem. Phys. **150**, 074110 (2019).